J Mater Sci (2010) 45:1715–1724
DOI 10.1007/s10853-009-4108-1

Enhanced thermal stability in K_2O-metakaolin-based geopolymer concretes by Al_2O_3 and SiO_2 fillers addition

**E. Kamseu · A. Rizzuti · C. Leonelli ·
D. Perera**

Received: 4 June 2009 / Accepted: 3 December 2009 / Published online: 20 January 2010

Abstract Based on the principle of stability of geopolymer gel as refractory binder, a geopolymeric paste in the $K_2O–Al_2O_3–SiO_2$ system was developed and used to produce refractory concretes by adding various amount of α-quartz sand (grain size in the range 0.1 μm to 1 mm) and fine powder alumina (grain size in the range 0.1–100 μm). The consolidated samples were characterized before and after sintering using optical dilatometer, DSC, XRD and SEM. The total shrinkage in the range of 25–900 °C was less than 3%, reduced with respect to the most diffused potassium or sodium based geopolymer systems, which generally records a >5% shrinkage. The maximum shrinkage of the basic geopolymer composition was recorded at 1000 °C with a 17% shrinkage which is reduced to 12% by alumina addition. The temperature of maximum densification was shifted from 1000 °C to 1150 or 1200 °C by adding 75 wt% α-quartz sand or fine powder alumina respectively. The sequences of sintering of geopolymer concretes could be resumed as dehydration, dehydroxylation, densification and finally plastic deformation due to the importance of liquid phase. The geopolymer formulations developed in this study appeared as promising candidates for high-temperature applications: refractory, fire resistant or insulating materials.

E. Kamseu (✉) · A. Rizzuti · C. Leonelli
Department of Materials and Environmental Engineering,
University of Modena and Reggio Emilia, Via Vignolese 905,
41100 Modena, Italy
e-mail: elie.kamseu@unimore.it; kamseuelie2001@yahoo.fr

D. Perera
School of Materials Science and Engineering, University of New
South Wales, Sydney, NSW 2052, Australia

Introduction

The current and potential applications for geopolymer materials have been mentioned in the literature, for e.g. Perera [1], and the uses are listed as fire resistance panels, low-temperature refractories, tooling for foundry industry, insulating components, hazardous and nuclear waste immobilization, biomaterials, building materials, etc. The basic advantage of geopolymers is the processing time which make the materials set very rapidly while still attaining final mechanical properties as well as having thermal and chemical resistance.

The material is produced through sequences of low-temperature physico-chemical reactions with hydroxide molecules that remain in the structure of the final product till about 500–600 °C [2–4]. Several workers have investigated metakaolin-based geopolymers activated using potassium and/or sodium alkali for high-temperature applications [5–10]. For use as a ceramic for high-temperature applications, geopolymers made from potassium are better than those from sodium [2]. The common compositions in the literature [1–5] contain important proportion of alkali that contribute to lowering the temperature of densification of the products of geopolymerization by developing eutectic. Amongst the alkali solutions, that of potassium and cesium have been identified to be suitable for the high-temperature geopolymer products [5, 10].

Geopolymers for high-temperature applications required fully dehydrated geopolymeric gel containing a greater proportion of aluminol groups [5, 6, 10]. Higher extents of consolidation at low temperature make the gel more rigid and unable to relax as effectively, thus only a slight reduction of dimension should be observed for geopolymers before the temperature of densification of the corresponding $M_2O–Al_2O_3–SiO_2$ systems [10]. Moreover, for the case of geopolymers for high-temperature applications, it is convenient to develop compositions with low shrinkage for the suitable behavior of material in service. For this, addition of fillers that can reduce shrinkage seem to be indicated as in usual ceramic matrix composites. Suitable study of thermal behavior for the appropriate composition for each specific application in addition to the prediction of their behavior in thermo-reactive environment should help.

In the literature, several authors [1, 7–10] explored some basic aspects of the geopolymer materials exposed to elevated temperatures. They estimated the structure stable enough to resist to exposure to high temperatures. Duxson et al. [10] observed little change in XRD and NMR structure up to 1400 °C but we should note that the shrinkage due to dehydration and dehydroxylation as well as structural reorganization occurs in the M_2O–Al_2O_3–SiO_2 systems due their ability to form eutectic as low as 900 °C [5, 6]. Therefore, geopolymer compositions for high-temperature applications should be monitored in the direction in which the formation of liquid phase is minimized. Even though the XRD and NMR the mineralogical composition do not significantly change up to 1400 °C [10], the dissolution of grains by liquid phase formed and the development of cracks, above 1200 °C, are both subjects of interest for the development of geopolymer for high-temperature applications. It is now evident how the knowledge of geopolymer transformation from room temperature till 1200 °C is critical for high-temperature applications, which means that a study of the sintering behavior of geopolymer is necessary to predict the route of production of the required structure in order to control its physico-chemical and physico-mechanical behavior in services [11].

A most promising approach of sintering is connecting with the use of continuum mechanics, which has been successfully applied to the description of compaction of porous bodies and it is based upon the theories of plastic deformation of porous bodies [12]. One of the most characteristic parameters inherent to the sintering phenomena is a change of dimensions of a porous body. This enable analysis of sintering as a macroscopic process of volume and shape deformation caused by substance flow of porous body skeleton. Sintering typically relies on surface energy as a primary driving force for particle bonding and densification. Surface tension contributes to a weak sintering stress that couples with atomic motion to form interparticle bonds. Because the sintering stress is low, most materials require a high temperature to induce significant flow to obtain measurable shrinkage. However, gravity force provides another fundamental stress that acts on the material during sintering. Unfortunately, gravity is not isotropic, so it induces anisotropic deformation and contributes to non-uniform shrinkage, microstructure gradients, and compact slumping [12, 13].

It has been demonstrated that dimensional changes can be controlled by monitoring the phase compositions in the final product [14]. If the dimensional changes of geopolymer are measured during sintering, the material will shrink normally until it is close to the point at which sufficient thermal energy is available for the molecules to rearrange themselves into more dense structure having smaller volume [15]. In their study of thermo-mechanical and microstructure of Na-geopolymers, Van Riessen [6] found that the shrinkage remains constant up to 800 °C after a peak of dehydration/dehydroxylation at 250 °C. K-geopolymers developed shrinkage >5% already in the 25–600 °C range and at 800 °C the rate of densification increase dramatically [8]. The resistance to densification and distortion goes down with an increase in the liquid content if there is a decrease in the connectivity and increase in liquid film thickness. The grain coarsening and the resulting liquid film coarsening cause a drop in the microstructural rigidity. The principle of geopolymerization is based on the dissolution-precipitation and polycondensation in which alkali ions play a particular role. The presence of alkali metal oxides is especially deleterious to the production of strong Al_2O_3–SiO_2 systems. Hence, it is critical to choose the correct amount of alkali in relation to the Al/Si ratio of the geoplymer matrix to reach good thermal resistance. The aim of this work is to study the effect of added phases, silica or alumina, on the sintering behavior of geopolymer matrices for applications at high temperature. The starting geopolymer formulation with the optimized potassium content is reported elsewhere [16, 17]. Apart from the scanning calorimetry (DSC), optical dilatometer was used with the possibility to follow-up the sample during characterization. The precision and the reproduction of data collected with a non-contact dilatometer have been already demonstrated [16, 17] and are here applied to the thermal characterization of geopolymers. Moreover, phase evolution and microstructural transformation were followed with x-ray diffraction (XRD) and scanning electron microscopy (SEM) observations.

Materials and methods

Materials and samples preparation

High-purity grade of kaolin (Colorobbia, Italy) was calcined for 6 h at 700 °C and ground under 100 μm. The metakaolin obtained has a SiO_2:Al_2O_3 ratio of 2.14. The geopolymer gel was prepared by dissolving suitable amount of metakaolin in a potassium hydroxide/potassium silicate solution (volume ratio 1:1). The potassium hydroxide (reagent grade, Carlo Erba, Italy) has a concentration of ~8 M and the potassium silicate (KS19-41 from Ingessil, Italy) has a SiO_2/K_2O molar ratio of 3.01 and a density of 1.38 g/cm^3. The suspension was ball-milled in porcelain jars for 5 min (1500 rpm). The geopolymer gel was used to prepare six samples of geopolymer refractory concrete by adding different proportion of alumina (0.1–100 μm grain size range, corundum crystalline phase) and silica sand (100 μm to 1 mm grain size range, α-quartz crystalline phase). These series of samples were designated RGP-A and RGP-S respectively as presented in Table 1. One sample free of additive was also made (RGP-K). The formulae shown in Table 1 were converted in weight percent to adapt the compositions of geopolymer concretes to the K_2O–Al_2O_3–SiO_2 ternary diagram [18] (Fig. 1).

Table 1 Composition of samples of geopolymer materials

Sample	KOH/K_2SiO_3 (vol.)	Liquid/solid (wt)	Chemical formula of geopolymer concretes
RGP-K	1:1	0.80	$K_2O{\cdot}2.55Al_2O_3{\cdot}7.36SiO_2$
RGPS4	1:1	0.72	$K_2O{\cdot}2.55Al_2O_3{\cdot}10.07SiO_2$
RGPS2	1:1	0.60	$K_2O{\cdot}2.55Al_2O_3{\cdot}12.77SiO_2$
RGPS34	1:1	0.51	$K_2O{\cdot}2.55Al_2O_3{\cdot}15.47SiO_2$
RGPA4	1:1	0.72	$K_2O{\cdot}4.14Al_2O_3{\cdot}7.36SiO_2$
RGPA2	1:1	0.60	$K_2O{\cdot}5.72Al_2O_3{\cdot}7.36SiO_2$
RGPA34	1:1	0.51	$K_2O{\cdot}7.32Al_2O_3{\cdot}7.36SiO_2$

The highly viscous slurries were poured into plastic moulds with 7–10 mm height and 40 mm diameter. All the samples were sealed in a plastic envelope and cured at ambient temperature for 24 h. After demoulding, the samples were conserved in air for final drying.

Thermal characterization of samples of geopolymer concretes

The geopolymer refractory concretes obtained were sintered in an electric muffle kiln at 200, 800 and 1000 and 1200 °C for 4 h in air and naturally cooled to room temperature. Contactless optical dilatometry (ESS MISURA HSM ODHT model 1600/80, Expert System, Modena, Italy) measurements were performed on shaped geopolymer concretes (5 × 5 × 15 mm^3) up to 1300 °C. The measurements were conducted under the same heating conditions (10 °C·min^{-1}) for all the samples.

Standard thermal analysis instrument (model DSC 404, Netzsch, Germany) was used for DSC analysis. The operating conditions were 0–1300 °C at 10 °C·min^{-1} for all the samples. For this analysis, samples of geopolymer concretes were ground to fine powders and platinum crucible was used as a sample holder.

Fig. 1 Ternary phase diagram of K_2O–Al_2O_3–SiO_2 (adapted from Osborn and Muan [28]) showing the compositions of geopolymer concretes; the concentration scale is in weight percent

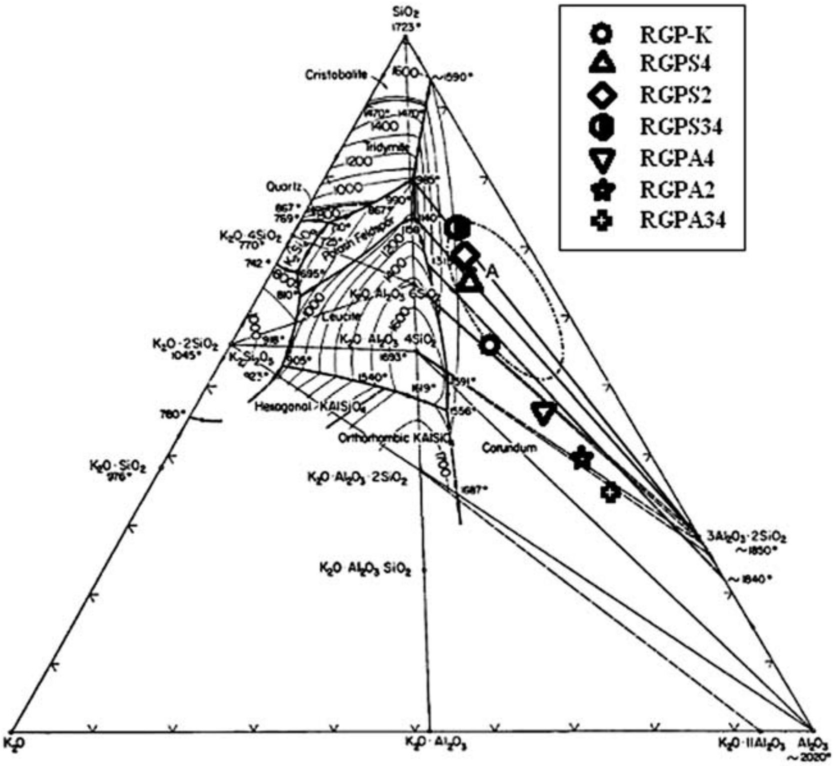

XRD and microstructure

XRD of fired specimens was analyzed with Ni filtered CuKα radiation using a Bragg-Brentano goniometer (model PW3050/60, Panalytical). The diffractometer was set at 40 kV (theta/theta) and 40 mA. During data collection, the 2θ step size was 0.02°, the counting time was 3 s in the range between 5 and 70°. XRD was performed on fine ground powder of fired geopolymer concretes. The microstructure of the fired specimens was studied by SEM (mod. XL40, Philips, The Netherlands). Freshly fractured surfaces and freshly fractured polished specimens were used for each sample. The polished specimens were etched in 5% HF-HNO_3 solution for 30 s for crystalline phase identification. All the specimens for SEM analysis were mounted on aluminum stubs and sputter-coated with 10 nm of Au/Pd to facilitate imagining. The microanalysis was performed using EDS (X_EDS INCA, Oxford Inst.).

Results and discussion

Dehydration and dehydroxylation

In our previous study [16, 17], we investigated and compared the sintering behavior of Na and K geopolymer formulations. The K-geopolymer, with composition corresponding to the RGP-K of this study, presents an endothermic peak below 200 °C which was ascribed to the loss of water, corresponding to an average value of 9% of loss of ignition. After the loss of the adsorbed water, the K-geopolymer presented continuous and slow dehydroxylation as well as densification with an exothermic peak which appear around 990 °C. Such a peak was attributed to structural reorganization [19].

By progressively adding silica sand or alumina as fillers in RGP-K formulation, the release of adsorbed water was not strongly influenced and no significant variation of shrinkage phenomena was observed up to 110 °C, where the dimensional changes were almost zero (Fig. 2a, b). This can be explained by taking into account that the capillary strain from dehydration is not yet sufficient to make the material shrink. From 110 to 500 °C, progressive dehyroxylation was at the origin of shrinkage. At 500 °C, the shrinkage was 2.26, 2.01, 1.8 and 1.33% for 0, 25, 50 and 75 wt% of addition of fine SiO_2 sand, respectively. These values remain constant up to 884 °C for RGP-K. For RGP-S4, RGP-S2 and RGP-S34 no variation was observed up to 872, 887 and 901 °C, respectively (Fig. 1a). Similar study exhibited shrinkage around 2% from 200 °C up to 750 °C [6] and >5% right from 600 °C [10], for both samples the densification temperature was 800 °C. The shrinkage behavior of the two compositions could be easily correlated to the Si/Al ratios [6, 10].

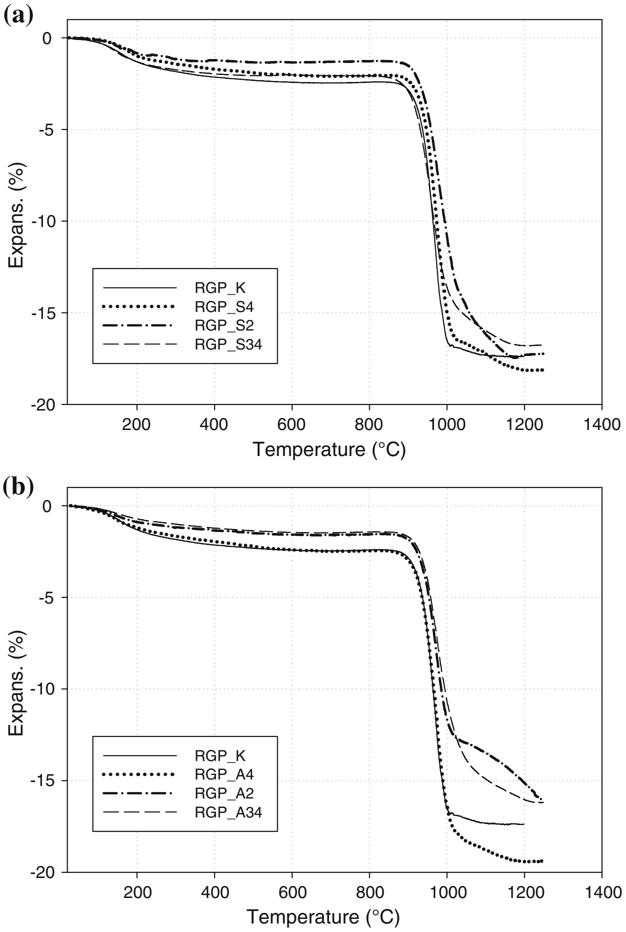

Fig. 2 Optical dilatometry curves of geopolymer concretes with **a** 0% (RGP-K), 25% (RGP-S4), 50% (RGP-S2) and 75% (RGP-S34) of sand addition and **b** 0% (RGP-K), 25% (RGP-A4), 50% (RGP-A2) and 75% (RGP-A34) of alumina addition

When alumina was added in place of silica sand, with the same percentages, the shrinkage goes from 0 at 110 °C to 2.2% at 495 °C and remain constant up to 884 °C for RGP-A4 with 25 wt% of alumina. Constant shrinkage was observed earlier in RGP-A2 and RGP-A34 samples, i.e. starting from 405 °C with 1.27 and 1.15%, respectively (Fig. 2b). The corresponding maximum temperatures at which the shrinkage remain unchanged were 892 and 896 °C, respectively. These observations indicate that apart from dehydration and dehydroxylation, there was no additional important transformation during the thermal treatment of geopolymer refractory concretes up to 900 °C.

The effect of additives, silica or alumina, on the thermal events recorded in the DSC curves is reported in Fig. 3. Independently of the composition, endothermic peaks, observed between 100 and 250 °C, should be undoubtedly ascribed to the phenomena of dehydration and

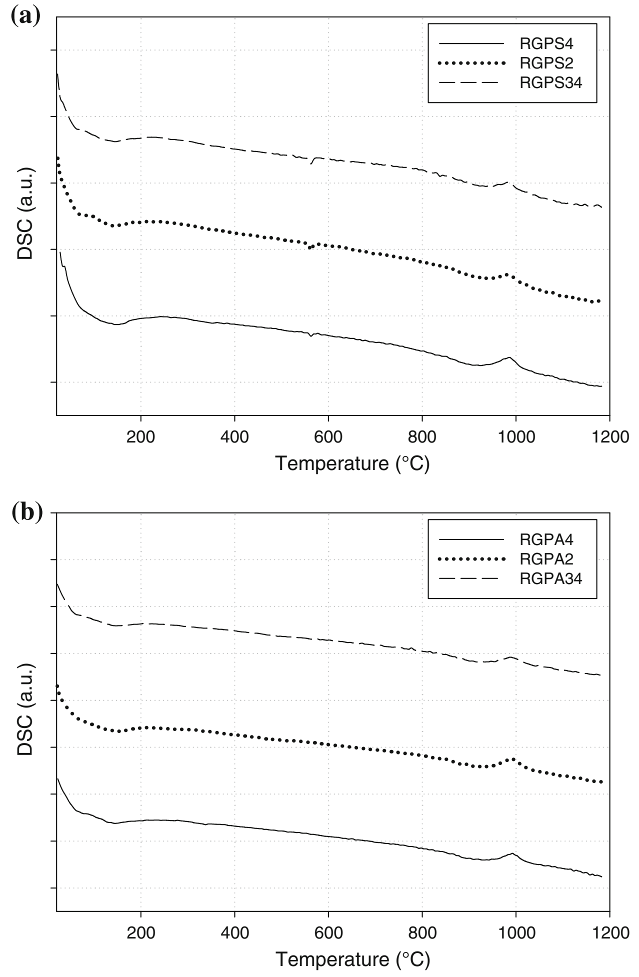

Fig. 3 DSC curves of geopolymer concretes with **a** 0% (RGP-K), 25% (RGP-S4), 50% (RGP-S2) and 75% (RGP-S34) of sand addition and **b** 0% (RGP-K), 25% (RGP-A4), 50% (RGP-A2) and 75% (RGP-A34) of sand addition

dehydroxylation. In particular, when SiO_2 is added, from 250 to 918 °C for RGP-S4, 926 °C for RGP-S2 and 953 °C for RGP-S34 no important transformation is identified if we do not consider the quartz transition that take place at 560 °C for all the three compositions (Fig. 3a). This peak is evidently ascribed to the alpha to beta-quartz phase transition. The same observation was not possible for sample with alumina addition (Fig. 3b). In this case, endothermic reactions due to water release from ambient to 250 °C can be compared to the results of Fig. 3a. In fact, Fig. 3b shows no physico-chemical transformation of great importance up to 956, 948 and 961 °C for RGP-A4, RGP-A2 and RGP-A34, respectively, indicating for alumina a higher refractory activity than for silica.

According to literature, the final products of geopolymerization contain physically bonded water, chemically bonded water and hydroxyl groups (OH) [20–23]. From the experimental data discussed above, the shrinkage begins after 110 °C, for RGP-S and RGP-A samples, and continues as result of progressive evaporation of the absorbed and weakly bound water up to approximately 250 °C (end of the endothermic peak). Up to the temperature that characterizes the end of the endothermic peaks (250 °C), dehydration and dehydroxylation make the shrinkage reach an average value of only 1% for the geopolymer concretes under study. Results presented in the literature [6, 10, 20] confirm the relative thermal stability after dehydration due to the low shrinkage in the region characterized by the slow dehydroxylation of hydroxyl groups. This is exactly what is observed in Figs. 2 and 3, where above 250 °C, there is a small densification which continues up to 900 °C, indicating a good thermal stability of all the formulations tested. From the results obtained we comment that alumina or silica sand can be used to control the shrinkage (dehydration and dehydroxylation) with the aim to control the properties at high temperatures.

Densification, deformation and cracks propagation

The exothermic peaks at 994 °C for RGP-A4, 988 °C for RGP-A2 and RGP-A34 (Fig. 3b) are indicative for the structural reorganization of the samples. Similar observations can be made on Fig. 2a for the samples with sand addition. The peaks appear at 994 °C for RGP-S4, 991 °C for RGP-S2 and 988 °C for RGP-S34. These peaks can be compared to peaks of crystallization of mullite that generally appear during the sintering of kaolin [19]. In this case, the peak is less significant with respect to the peak of crystallization in pure kaolin as a consequence of the formation of polymeric gels that engages Al and Si ions, responsible for the mullitization. If we consider the unreacted metakaolin (due to insufficient or partial dissolution in the alkali solution) that can be converted to mullite, further characterization should be made to confirm the presence of such crystalline phase since XRD patterns do not confirm the presence of mullite. By the way we ascribed the exothermic peak of Fig. 3 to structural reorganization.

The peak of structural reorganization (Fig. 3a, b) corresponds to the point of major particles packing for all the samples (Fig. 2a, b). In order to provide more evidence for this conclusion, the densification rate is reported in Fig. 4a, b. The domain of densification detailed in Fig. 4 correspond exactly with the domain of exothermic peaks (Fig. 3) that is characteristic of the structural reorganization considering the DSC analysis. The respective peaks of structural reorganization described above fitted with the region of major densification (975–1000 °C) as it can be observed in Fig. 4. Between 880 and 1015 °C, RGP-K goes from 2.4 to 16.8% of shrinkage. For the samples with sand addition, the maximum shrinkage was recorded

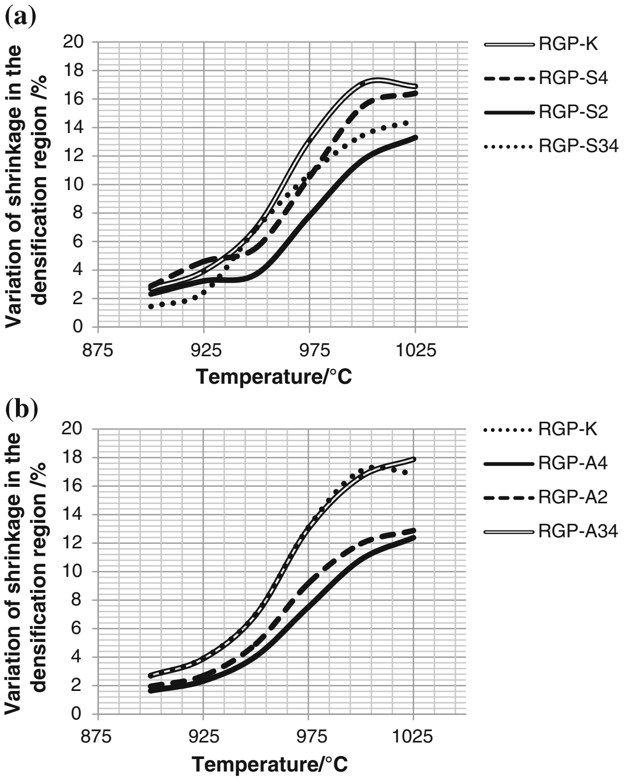

Fig. 4 Variation of linear shrinkage in the region of densification of **a** sand-rich geopolymer concretes and **b** alumina-rich geopolymer concretes

to be 16.27, 14.54 and 13.25% at the same temperatures as the DSC exothermic peak for RGP-S4, RGP-S2 and RGP-S34, respectively. With addition of alumina, the shrinkage at 1015 °C was 17.6% for RGP-A4, 12.75% for RGP-A2 and RGP-A34. Davidovits [20] explained that complete dehydration results in irreversible shrinkage as a consequence of the changes in the framework, which stabilize the geopolymer towards further heat treatment. Once stabilized, i.e. after dehydroxylation and shrinkage, the geopolymeric products follow the classical thermal history of ceramics.

In this work, we have tried to ameliorate the behavior of the geopolymer at high temperatures by adding refractory fillers to reduce the strain and cracks that result from the typical amorphous structure of the standard compositions of geopolymer. The first results are the increase of the temperature at which shrinkage occurs in geopolymer materials during sintering. The densification in this case was shifted from 800 °C to around 1000 °C as compared to the results already obtained from the thermal behavior of (Na, K)-geopolymers [6, 10]. The shrinkage remains under control up to 900 °C and it is reduced to about 3%. So for these formulations it is possible to speak about geopolymer concretes with temperature of application up to 1000–1100 °C. The densification curves (Fig. 4a, b) up to these ranges of temperatures can be compared to the master sintering curves of conventional ceramic with liquid phase sintering [24]. After these temperatures, even though there is in the literature, assertion about the stability of the geopolymer structure up to 1400 °C [14, 21, 22], the dissolution of grains by liquid phase formed, mainly in sand added concretes, and development of cracks after 1200 °C seem to state the limits of application. During geopolymerization, the potassium hydroxide solution as well as the potassium silicate solution governs the dissolution and polycondensation phenomenon being responsible of the reticulation and strength of the matrix composite. But composition of the K_2O–Al_2O_3–SiO_2 systems will develop liquid film starting from 900 °C. With the temperature increase, when more liquid is formed, the matrix is progressively attacked. The interactions of liquid phase and matrix will be at the origin of multiple tensions [5, 15]. These tensions that are due to the development of sintering stress and the difference in coefficient of thermal expansion between the liquid phase and the matrix are at the origin of cracks, strong shrinkage and deformations observed for the samples under study. The geopolymer concretes after dehydration and dehydroxylation see their porosity reduced and by the way the densification increases. The addition of silica sand contributes to the limitation of sintering stresses in the matrix with temperature development but increases the densification of the geopolymer materials when the liquid phase is present due to the possible dissolution as compared to the calcined alumina. Structural densification occurs when the softening temperature of the material is reached, and the viscous sintering begins to contribute to shrinkage, since the structure is able to move more freely [15, 25]. From Fig. 1, the addition of silica sand contributes to orient the composition of geopolymer concretes through region of refractory silicates. However, the reinforcements as used for geopolymer concretes are discontinued and do not insure the homogeneity of the matrix. The cracks as observed are the product of thermal expansion anisotropy between high refractory grains of fillers and amorphous polysialate phases with high concentration of potassium ions. When the liquid is formed at temperature >1200 °C, the region shrink differently which at the end result in microcraks and possible cracks growth that will be responsible for the poor properties. This situation is not similar with alumina addition. Referring to the ternary phase diagram, it can be observed that region of high concentration of alumina in $K_2OAl_2O_3SiO_2$ system will develop more refractoriness. Moreover, the interfaces between the matrix of geopolymer and alumina grains at high temperature seem to be more stable.

Phase evolution and microstructure

XRD patterns of geopolymer concretes show them as amorphous matrix in which additional α-quartz for sand-rich and corundum for Al-rich are embedded (Fig. 5). The amorphous nature of K-geopolymer has already been demonstrated by Kriven et al. [23]. The principal phases that are expected in the fully reacted K-geopolymer are kalsilite K[$AlSiO_4$] and kaliophilite [$KAlSiO_4$] embedded in an amorphous matrixes [23, 26]. Figure 5a, b shows the phase evolution from XRD patterns of geopolymer concretes under study as a function of temperature. For RGP-S samples, the intensity of quartz increases with the percentage of addition of α-quartz sand and the amorphous structure remain up to 800 °C. A similar situation is observed for Al-rich geopolymer concretes. The XRD patterns of K-geopolymer investigated in the previous work demonstrated the conservation of structure of the material up to 900 °C [16, 17]. Increasing the temperature above 800 °C, the principal feature of the XRD pattern is the increase of the crystallinity of the samples with the amorphous structure disappearing. K-geopolymers are expected to develop leucite and potassium nepheline with temperature, the content increases gradually starting from 800 °C [10]. Kriven et al. [23] described K-polysialate as nanoparticles separated by nanoporosity with sponge-like microstructure characterized by fully dense regions that remain amorphous up to 1000 °C. Leucite crystallized as the major phase after being heated to >1000 °C, although minor kalsilite was also formed [26]. In this work, we used

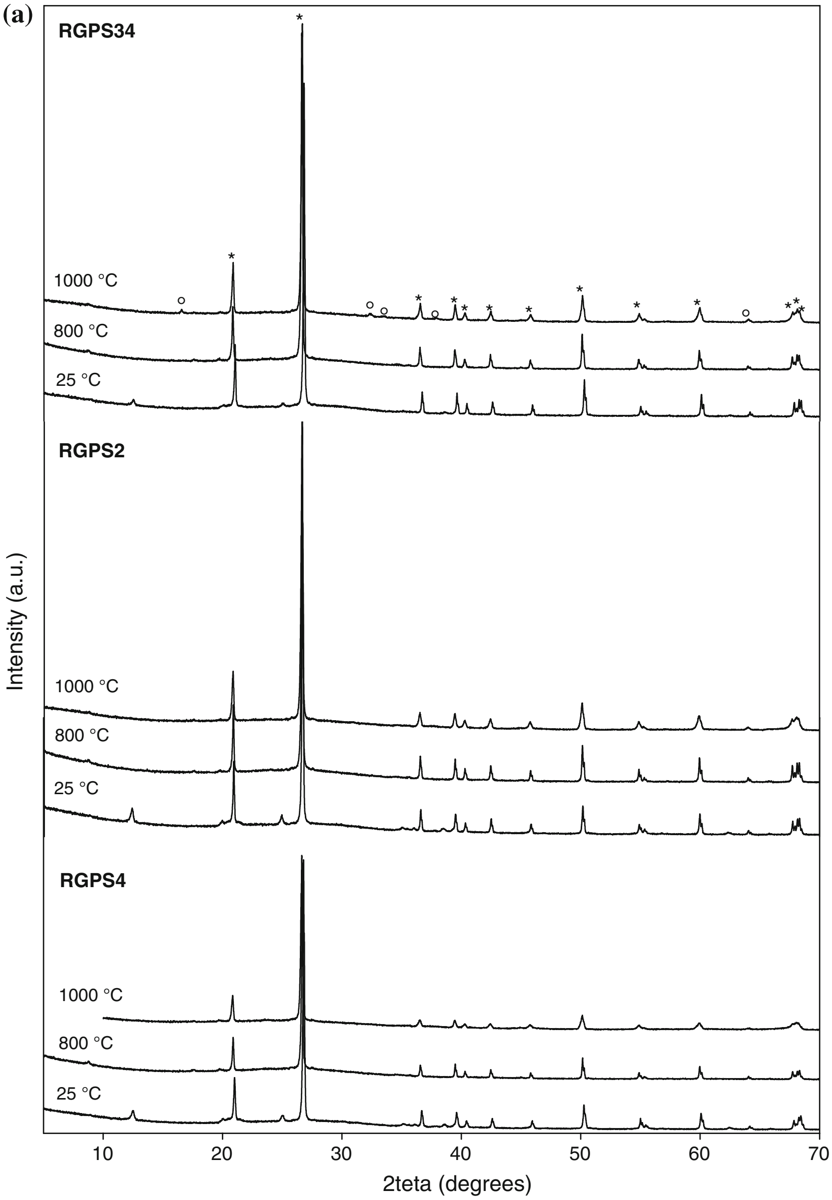

Fig. 5 XRD patterns of geopolymer concretes with **a** 0% (RGP-K), 25% (RGP-S4), 50% (RGP-S2) and 75% (RGP-S34) of sand addition at 25, 800 and 1000 °C and **b** 0% (RGP-K), 25% (RGP-A4), 50% (RGP-A2) and 75% (RGP-A34) of sand addition at 25, 800 and 1000 °C

Fig. 5 continued

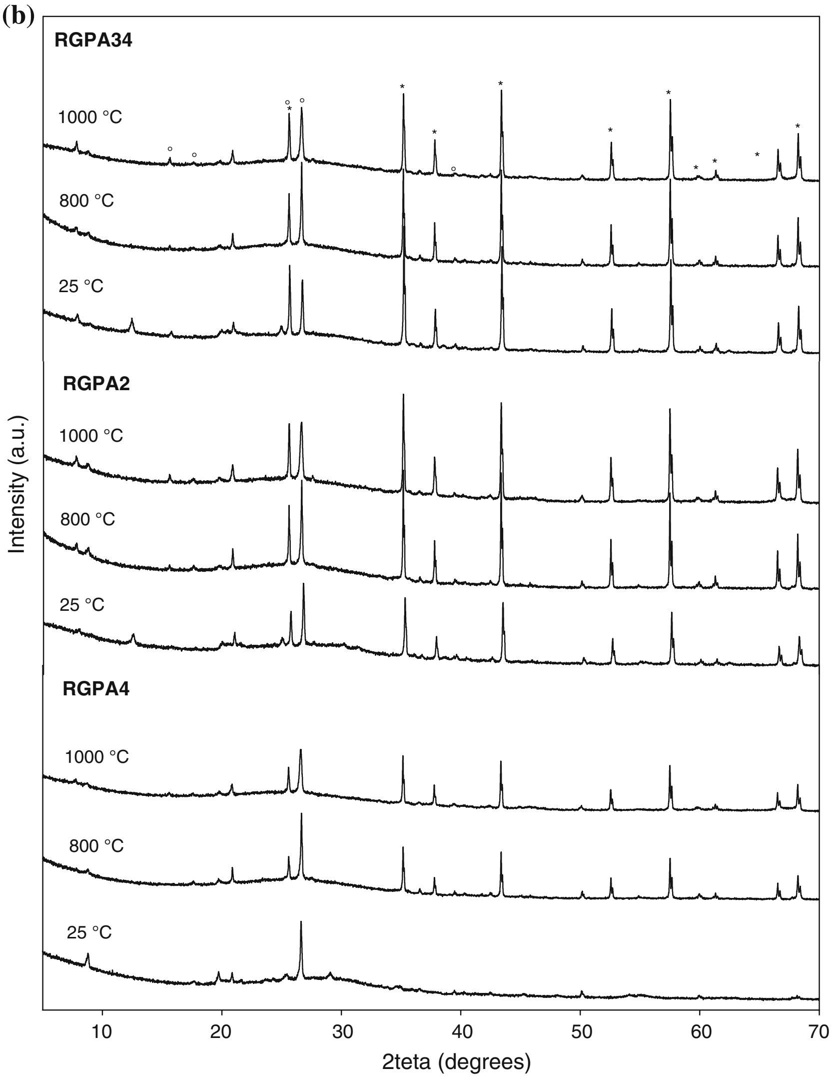

α-quartz sand and alumina as fillers with the expectancy that fine nanosized particles of the metakaolin will act as seeders during geopolymerization [27] while the relative coarse particles of the two fillers will only partly react with the remaining alkali-ions. As consequence, the vitrification is postponed to high temperature (Fig. 2). The development of crystalline phases between 800 and 1000 °C can explain the major densification that is combined with shrinkage observed for all the samples. The relative decrease in intensities of peaks of crystalline phases should be ascribed to the appearance of the liquid phase in the matrix. The liquid will affect crystalline phases, such as quartz, by partial dissolution (Fig. 5). The development of crystalline phases during thermal treatment of geopolymer concretes was found to be influenced not only by the intrinsic ability of K-polysialates to convert to crystalline phases (leucite, kalsilite, etc.) but also by the nature and the amount of fillers. Al-rich geopolymer concretes act more efficiently with respect to sand-rich geopolymers.

Perera et al. [13] observed in their study on development of refractory castables that K-geopolymers mineral phases were maintained from ambient temperature to 800 °C. At 1000 °C, kaliophilite was the major phase in replacement of the originally amorphous phase. From 1200 °C, quartz disappeared as a consequence of the presence of liquid phase. The presence of distorted kalsilite, leucite as well as liquid phase was responsible for the deformation observed. Even though kalsilite and leucite have melting points at 1750 and 1686 °C, respectively, the resistance at high temperature of RGP-S and RGP-A was due mostly to fillers that act as inhibitors of liquid phase development and retard the densification of the matrix (Figs. 2 and 6). The maximum shrinkage of the K-geopolymer was recorded around 1000 °C with a 17% shrinkage which is reduced to 12% only by alumina addition. The temperature at which

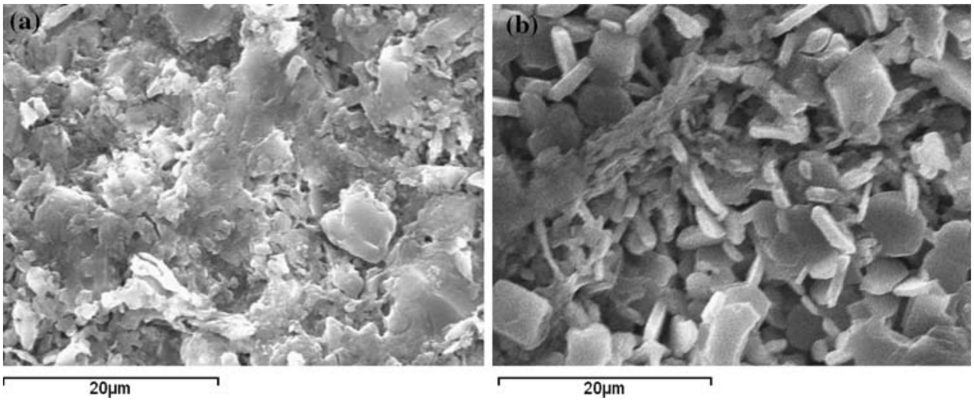

Fig. 6 SEM micrographs of **a** RGP-S2 and **b** RGP-A2 at 1000 °C showing (after etching) good densification with various crystalline phases responsible of the refractoriness

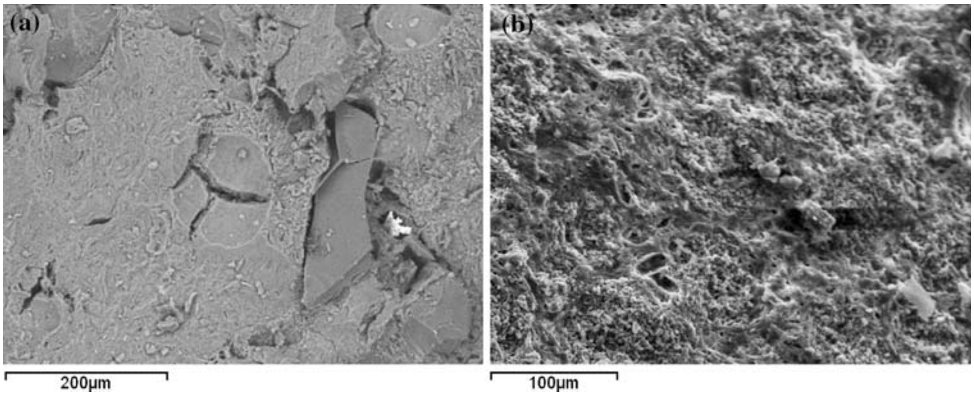

Fig. 7 Fracture surface of geopolymer concretes (**a** Si-rich; **b** Al-rich) at 1200 °C showing the influence of liquid phase and thermal expansion mismatch on the microstructure

samples of RGP showed constant shrinkage following densification was shifted from 1000 °C to 1150 or 1200 °C by adding 75 wt% α-quartz sand or fine powder alumina, respectively. The presence of only kalsilite and leucite (even though it was not easier to identify these phases in this work) in the matrix of K-geopolymers, taking into account the proportion of alkali in the bulk composition, seem to be not enough to inhibit the formation of significant amount of liquid phase. Liquid phase is detrimental for the crystallization during sintering. Even with the addition of fillers, the ratio of geopolymer paste/filler has to be optimized so that the mechanical properties of the final product can remain under control. Increasing the temperature above 1200 °C, the equilibrium is interrupted, thus cracks, deformation and shrinkage contribute to bring down the properties of geopolymer concretes. This is much more important for sand-rich than alumina-rich geopolymer concretes (Fig. 7).

Conclusion

Geopolymer refractory concretes were prepared by reinforcing the matrix of K_2O–Al_2O_3–SiO_2 polysialate systems with α-quartz or alumina. Under thermal treatment, dehydration, dehydroxylation, densification and deformation remain the principal sequences of sintering. The products obtained developed up to 900 °C shrinkage under 3%. The total shrinkage was shifted from 17% at 1000 °C for the basic K-geopolymer paste to 12 and 13% by adding alumina or quartz, respectively. Addition of fillers permitted to shift the densification temperature compared to conventional geopolymer compositions. The presence of fillers acted as additional effect to crystalline phases (kalsilite and leucite) for the inhibition of the development of liquid phase. The presence of microcracks from 1200 °C suggested the presence of sintering stresses due to the gradient between the matrix and the new liquid phase produced. Geopolymer concretes seem to be suitable for thermal applications up to 1100 °C. The thermal behavior of the obtained products presented them as promising candidates as geopolymer compositions for high-temperature applications. But there is still need to complete the investigation with mechanical behavior and porosity.

Acknowledgement We are particularly grateful to Dr. Braga Mirko, R&D Laboratory, INGESSIL S.r.l., (Verona, Italy) for providing the potassium silicate solution.

References

1. Perera DS (2007) In: Cook R, Coyle T, Fischman G, Hellmann J, Green M, Hobbs L, Logan K, Sideridis C, Singh M, Smith J (eds) Global roadmap for ceramics and glass technology. Wiley-Interscience, New York, pp 623–634

2. Barbosa VFF, Mackenzie KJD (2003) Mater Letter 57:1477
3. Van Deventer JSJ, Provis JL, Duxson P, Lukey GC (2007) J Hazard Mater A139:506
4. Xu H, Van Deventer JSJ (2000) Int J Miner Process 59:247
5. Rahier H, Van Mele B, Wastiels J (1996) J Mater Sci 31:80. doi:10.1007/BF00355129
6. Van Riessen SA (2007) J Mater Sci 42:3117. doi:10.1007/s10853-006-0522-9
7. Richard WDA, Van Riessen SA, Walls P (2008) Int J Ceram Tech 1–8
8. Perera DS, Trautman RL (2005) Adv Tech Mater Mater Process J 7(4):187
9. Duxson P, Lukey GC, Van Deventer JSJ (2006) J Non-Cryst Solids 352(52–54):5541
10. Duxson P, Lukey GC, Van Deventer SJJ (2007) J Non-Cryst Solids 353(22–23):2186
11. Perera DS, Vance ER, Cassidy DJ, Blackford MG, Hanna JV, Trauman RL, Nicholson CL (2004) Ceram Trans 165:87
12. Svoboda J, Riedel H (1995) Acta Metall 43(1):1
13. Savitskii AP (1991) Liquid phase sintering of the systems with interacting components. Russian Academy of Sciences
14. Maiti KN, Kumar S (1992) Br Ceram Trans J 91(1):19
15. Coble RL (1961) J Appl Phys 32:787
16. Kamseu E, Leonelli C, Perera D (2009) Ceram Trans (in press)
17. Olevsky EA, Rajendra Bordia (2010) Advances in sintering: ceramic transactions. American Ceramic Society, Westerville, OH. ISBN: 978-0-470-40849-0
18. Chakraborty S, Dingwell DB, Rubie DC (1995) Geochem Cosmochim Acta 59(2):255
19. Leonelli C, Kamseu E, Melo UC, Corradi A, Pellacani GC (2008) Interceram 57(6):396
20. Davidovits J (2008) Geopolymer chemistry and applications. Morrisville, USA, p 570
21. Perera DS, Vance ER, Finnie KS, Blackford MG, Hanna JV, Cassidy DJ, Nicholson CL (2006) Ceram Trans 175:225
22. Bakharev T (2006) Cem Concr Res 36:1134
23. Kriven WM, Bell J, Gordon M (2003) Ceram Trans 153:227
24. Kiani S, Panw J, Yeomans JA (2006) Am Ceram Soc 89(11):3393
25. Delale F, Boduroghu H (1991) Eng Fract Mech 39(1):45
26. Bell JL, Driemeyer PE, Kriven WM (2009) J Am Ceram Soc 92(3):607
27. Ress CA, Provis JL, Lukey GC, Van Deventer JSJ (2008) Colloids Surf A Physicochem Eng Asp 318:97
28. Osborn EF, Muan A (1960) Phase equilibrium diagrams of oxide systems. The American Ceramic Society and The Edouard Orton Jr. Ceramic Foundation, Columbus, OH